

Super-spinning compact objects generated by thick accretion disks

Zilong Li and Cosimo Bambi¹

Center for Field Theory and Particle Physics & Department of Physics,
Fudan University, 220 Handan Road, 200433 Shanghai, China

E-mail: zilongli@fudan.edu.cn, bambi@fudan.edu.cn

Abstract. If astrophysical black hole candidates are the Kerr black holes predicted by General Relativity, the value of their spin parameter must be subject to the theoretical bound $|a_*| \leq 1$. In this work, we consider the possibility that these objects are either non-Kerr black holes in an alternative theory of gravity or exotic compact objects in General Relativity. We study the accretion process when their accretion disk is geometrically thick with a simple version of the Polish doughnut model. The picture of the accretion process may be qualitatively different from the one around a Kerr black hole. The inner edge of the disk may not have the typical cusp on the equatorial plane any more, but there may be two cusps, respectively above and below the equatorial plane. We extend previous work on the evolution of the spin parameter and we estimate the maximum value of a_* for the super-massive black hole candidates in galactic nuclei. Since measurements of the mean radiative efficiency of AGNs require $\eta > 0.15$, we infer the “observational” bound $|a_*| \lesssim 1.3$, which seems to be quite independent of the exact nature of these objects. Such a bound is only slightly weaker than $|a_*| \lesssim 1.2$ found in previous work for thin disks.

Keywords: modified gravity, accretion, astrophysical black holes.

¹Corresponding author

Contents

1	Introduction	1
2	The Polish doughnut model	2
3	Thick disks in non-Kerr space-times	4
3.1	Non-Kerr black holes in an alternative gravity theory	4
3.2	Exotic compact objects without horizon in General Relativity	6
4	Evolution of the spin parameter	7
5	Discussion	8
6	Summary and conclusions	10

1 Introduction

In 4-dimensional General Relativity, an uncharged black hole (BH) is described by the Kerr solution and it is completely specified by only two parameters: the mass M and the spin angular momentum J [1–3]. A fundamental limit for a Kerr BH is the bound $|a_*| \leq 1$, where $a_* = J/M^2$ is the BH spin parameter¹. For $|a_*| > 1$, there is no horizon, and the central singularity is naked, which is forbidden by the weak cosmic censorship conjecture [4]. Despite the apparent possibility of forming naked singularities from regular initial data [5], any effort to overspin an existing Kerr BH to $|a_*| > 1$ seems to be doomed to failure [6, 7], and, even if created, a Kerr naked singularity would be unstable and it should quickly decay [8, 9].

At the observational level, there are at least two classes of astrophysical BH candidates [10]: stellar-mass objects in X-ray binary systems ($M \approx 5 - 20 M_\odot$) and super-massive BH candidates at the center of every normal galaxy ($M \sim 10^5 - 10^9 M_\odot$). All these objects are thought to be the Kerr BHs predicted by General Relativity, but their actual nature has still to be verified [11, 12]. The Kerr paradigm requires $|a_*| \leq 1$, but such a bound may be violated if BH candidates are either non-Kerr BHs in an alternative theory of gravity or exotic compact objects in General Relativity. Several groups have recently put forwards different proposals to test the Kerr-nature of astrophysical BH candidates [13–29]. In general, there is a strong correlation between a_* and possible deviations from the Kerr geometry, in the sense that observations may not be able to distinguish a Kerr BH from a non-Kerr object with different a_* .

In this context, it is interesting to get an estimate of the possible range of the value of a_* . In Refs. [30, 31], it was shown that a thin accretion disk around a non-Kerr compact object can spin the body up to $|a_*| > 1$. In Ref. [32], it was presented an argument suggesting that the today spin parameters of the super-massive BH candidates at the centers of galaxies is likely smaller than 1.2, regardless of the exact nature of these objects. Future measurements of the radiative efficiency of AGNs may put stronger constraints on both the spin and the deformation parameter [33]. It has been also argued that rapidly-rotating non-Kerr BHs may have topologically non-trivial event horizons [34–36].

¹Throughout the paper, we use units in which $G_N = c = 1$.

In this work, we study the hydrodynamical structure of thick accretion disks in non-Kerr backgrounds. We consider the simplest case of a marginally stable disk in the framework of the Polish doughnut model [37, 38]. We show that the accretion process may be qualitatively different with respect to the Kerr case. The accretion disk may have two cusps, one above and one below the equatorial plane, and the gas of accretion may plunge from the cusps to the poles of the compact object. As in the Kerr background, the accretion process from a thick disk can be potentially more efficient than a thin disk to spin the central object up. We thus revise the result presented in Ref. [32], including the possibility that a super-massive BH candidate has experienced a period of super-Eddington accretion and that its current spin parameter still exceeds the equilibrium value for a thin accretion disk. The new bound on the spin parameter of the super-massive BH candidates is $|a_*| \lesssim 1.3$, only slightly weaker than the bound $|a_*| \lesssim 1.2$ found in [32].

The content of the paper is as follows. In Section 2, we review the Polish doughnut model and we discuss the possible accretion scenarios in the case of a Kerr background. In Section 3, we apply this model to describe the hydrodynamical structure of accreting disks around non-Kerr BHs in a putative alternative theory of gravity and to exotic compact objects in General Relativity. We find the same qualitative picture and we believe this is the general picture for non-Kerr backgrounds. In Section 4, we study the evolution of the spin parameter resulting from the accretion process as a function of the deformation of the compact object. The discussion of our result and the current spin measurements is reported in Section 5. If we assume a radiative efficiency $\eta > 0.15$, which is a conservative lower bound on the mean radiative efficiency of AGNs inferred by a few groups with the Soltan's argument, we find that the spin parameter of the super-massive BH candidates in galactic nuclei is $|a_*| \lesssim 1.3$. Summary and conclusions are reported in Section 6.

2 The Polish doughnut model

Geometrically thin and optically thick accretion disks around BHs are described by the Novikov-Thorne model [39], which is the relativistic generalization of the Shakura-Sunyaev model. Here, self-gravitation of the disk and gas pressure are neglected, so the fluid elements follow the geodesics of the background metric. The Novikov-Thorne model is thought to work for moderate accretion rates, when the accretion luminosity is between a few per cent to about 30% the Eddington luminosity of the object [40]. The Polish doughnut model was proposed in [37, 38] to describe non-self-gravitating disks when the gas pressure is not negligible. Because of the gas pressure, the disk can be geometrically thick and the fluid elements do not follow the geodesics of the background metric.

The Polish doughnut model requires that the space-time is stationary and axisymmetric. The line element can be written as

$$ds^2 = g_{tt}dt^2 + g_{rr}dr^2 + g_{\theta\theta}d\theta^2 + 2g_{t\phi}dtd\phi + g_{\phi\phi}d\phi^2, \quad (2.1)$$

where the metric elements are independent of the t and ϕ coordinates. The disk is modeled as a perfect fluid with purely azimuthal flow:

$$T^{\mu\nu} = (\rho + P)u^\mu u^\nu + g^{\mu\nu}P, \quad u^\mu = (u^t, 0, 0, u^\phi), \quad (2.2)$$

where ρ and P are, respectively, the energy density and the pressure. The specific energy of the fluid element, $-u_t$, its angular velocity, $\Omega = u^\phi/u^t$, and its angular momentum per unit

energy, $\lambda = -u_\phi/u_t$, are given by

$$u_t = -\sqrt{\frac{g_{t\phi}^2 - g_{tt}g_{\phi\phi}}{g_{\phi\phi} + 2\lambda g_{t\phi} + \lambda^2 g_{tt}}}, \quad \Omega = -\frac{\lambda g_{tt} + g_{t\phi}}{\lambda g_{t\phi} + g_{\phi\phi}}, \quad \lambda = -\frac{g_{t\phi} + \Omega g_{\phi\phi}}{g_{tt} + \Omega g_{t\phi}}. \quad (2.3)$$

Note that λ is conserved for a stationary and axisymmetric flow in a stationary and axisymmetric space-time [37]. The disk's structure can be inferred from the Euler's equations, $\nabla_\nu T^{\mu\nu} = 0$:

$$a^\mu = -\frac{g^{\mu\nu} + u^\mu u^\nu}{\rho + P} \partial_\nu P, \quad (2.4)$$

where $a^\mu = u^\nu \nabla_\nu u^\mu$ is the fluid's 4-acceleration. If the pressure is independent of the t and ϕ coordinates (which follows from the stationarity and axisymmetry of the background) and if the equation of state is barotropic ($\rho = \rho(P)$), a^μ can be written as a gradient of a scalar potential $W(P)$:

$$a_\mu = \partial_\mu W, \quad W(P) = -\int^P \frac{dP'}{\rho(P') + P'}. \quad (2.5)$$

After some algebra, one can see it is possible to express Ω as a function of λ , i.e. $\Omega = \Omega(\lambda)$, and integrate the Euler's equation to get W ²

$$W = W_{\text{in}} + \ln \frac{u_t}{u_t^{\text{in}}} + \int_{\lambda_{\text{in}}}^{\lambda} \frac{\Omega d\lambda'}{1 - \Omega\lambda'}, \quad (2.6)$$

where W_{in} , λ_{in} , and u_t^{in} are the potential, the angular momentum per unit energy, and the energy per unit mass at the inner edge of the fluid configuration. Here, W_{in} , λ_{in} , and u_t^{in} can be replaced by the value of W , λ , and u^t at any other point of the fluid's boundary. In the Newtonian limit, W reduces to the total potential, i.e. the sum of the gravitational potential and of the centrifugal one, and at infinity $W = 0$.

If the background metric is known, there is only one unspecified function, $\Omega = \Omega(\lambda)$, which characterizes the fluid's rotation. In the zero-viscosity case, this function cannot be deduced from any equation, and it must be given as an assumption of the model. Imposing a specific relation between Ω and λ , we can find the equipotential surfaces $W = \text{const.} < 0$, i.e. the surfaces of constant pressure, which represent the possible boundaries of the fluid configuration. One of these surfaces may have one (or more) sharp cusp(s), which may induce the accretion onto the compact object: like the cusp at the L_1 Lagrange point in a close binary system, the accreting gas can fill out the Roche lobe and then be transferred to the compact object. The mechanism does not need the fluid's viscosity to work, so the latter may be, at least in principle, very low.

A particularly simple case is the configuration with $\lambda = \text{const.}$, which is marginally stable with respect to axisymmetric perturbations (the criterion for convective stability is simply that λ does not have to decrease outward). In this specific case, the integral in Eq. (2.6) vanishes and

$$W = \ln(-u_t) + \text{const.} \quad (2.7)$$

In the Kerr space-time, we find five qualitatively different scenarios [38]:

²In the special case $\lambda = \text{const.}$, Ω is not constant, but Eq. (2.6) is still correct and the integral vanishes.

1. $\lambda < \lambda_{\text{ms}}$, where λ_{ms} is the angular momentum per unit energy of the marginally stable equatorial circular orbit (or innermost stable circular orbit, ISCO). No disks are possible, as there are no closed equipotential surfaces.
2. $\lambda = \lambda_{\text{ms}}$. The local minimum of W corresponding to the disk's center is located on the equatorial plane at the marginally stable radius. However, it is not really a minimum, but a flex. The disk exists as an infinitesimally thin unstable ring.
3. $\lambda_{\text{ms}} < \lambda < \lambda_{\text{mb}}$, where λ_{mb} is the angular momentum per unit energy of the marginally bound equatorial circular orbit. There are many stationary configurations without a cusp and one disk with a cusp on the equatorial plane, located between the marginally bound and the marginally stable radius. Accretion starts when the gas fills out all the equipotential surface with the cusp.
4. $\lambda = \lambda_{\text{mb}}$. The cusp is located on the equatorial plane and belongs to the marginally closed equipotential surface $W = 0$. Accretion is possible in the limit of a disk of infinite size.
5. $\lambda > \lambda_{\text{mb}}$. No accretion is possible, as there are no equipotential surfaces $W \leq 0$ with a cusp.

3 Thick disks in non-Kerr space-times

The Polish doughnut model is formulated for a generic stationary and axisymmetric space-time. In what follows, we apply this model to two non-Kerr backgrounds.

3.1 Non-Kerr black holes in an alternative gravity theory

The Johannsen-Psaltis (JP) metric describes non-Kerr BHs in a putative alternative theory of gravity. In its simplest version, the line element in Boyer-Lindquist coordinates reads

$$\begin{aligned}
 ds^2 = & - \left(1 - \frac{2Mr}{\Sigma} \right) (1+h) dt^2 - \frac{4aMr \sin^2 \theta}{\Sigma} (1+h) dt d\phi + \frac{\Sigma(1+h)}{\Delta + a^2 h \sin^2 \theta} dr^2 + \\
 & + \Sigma d\theta^2 + \left[\left(r^2 + a^2 + \frac{2a^2 Mr \sin^2 \theta}{\Sigma} \right) \sin^2 \theta + \frac{a^2 (\Sigma + 2Mr) \sin^4 \theta}{\Sigma} h \right] d\phi^2, \quad (3.1)
 \end{aligned}$$

where $a = a_* M$ and

$$\Sigma = r^2 + a^2 \cos^2 \theta, \quad \Delta = r^2 - 2Mr + a^2, \quad h = \frac{\epsilon_3 M^3 r}{\Sigma^2}. \quad (3.2)$$

The compact object is more prolate (oblate) than a Kerr BH for $\epsilon_3 > 0$ ($\epsilon_3 < 0$); when $\epsilon_3 = 0$, we recover the Kerr solution.

In the Kerr background, equatorial circular orbits are always vertically stable, while they are radially stable only for radii larger than the one of the marginally stable orbit. In a generic non-Kerr space-times, equatorial circular orbits may also be vertically unstable, which leads to a number of new phenomena [42, 43]. In the case of thick accretion disks in the JP background, we find two qualitatively different pictures which are related to the radial or vertical instability of the marginally stable orbit, even if the case of the transition space-times is less clear.

The ISCO is radially marginally stable when the central object is a Kerr BH ($\epsilon_3 = 0$), when it is more oblate than a Kerr BH ($\epsilon_3 < 0$), and also when it is more prolate than a Kerr BH and the spin parameter is below a critical value that depends on the deformation parameter ($\epsilon_3 > 0$ and $a_* < a_*^{\text{crit}}(\epsilon_3)$). The accretion process proceeds as described in the previous section and it is set by the value of λ with respect to the ones of λ_{ms} and λ_{mb} . The topology of the equipotential surfaces in the JP background with $a_* = 1.1$ and $\epsilon_3 = -1$ is shown in Fig. 1. There are no qualitative differences with the Kerr case (see Fig. 3 in [38]).

The second case, in which the marginally stable orbit is vertically unstable, occurs when the compact object is more prolate than a Kerr BH and its spin parameter is above a critical value ($\epsilon_3 > 0$ and $a_* > a_*^{\text{crit}}(\epsilon_3)$). Now, the space-time has no marginally bound orbit, as the marginally stable orbit is not a minimum of the particle energy. So, λ_{mb} cannot be defined. In addition to λ_{ms} , we find other two relevant values, say λ_1 and λ_2 , with $\lambda_1 < \lambda_{\text{ms}} < \lambda_2$. There are thus seven qualitatively different scenarios:

1. $\lambda < \lambda_1$ (Fig. 2, top left panel). No disks are possible, as there are no closed equipotential surfaces.
2. $\lambda = \lambda_1$ (Fig. 2, top right panel). There are two local minima of W , above and below the equatorial plane, corresponding to the two disks' centers. They are not really two minima, but two flexes. The disks exist as two infinitesimally thin unstable rings outside the equatorial plane.
3. $\lambda_1 < \lambda < \lambda_{\text{ms}}$ (Fig. 2, central left panel). There are two local minima of W , above and below the equatorial plane. We may have either two non-equatorial toroidal disks or one disk crossing the equatorial plane. There is one configuration with two cusps, which are located above and below the equatorial plane.
4. $\lambda = \lambda_{\text{ms}}$ (Fig. 2, central right panel). W has a local minimum located at the marginally stable orbit on the equatorial plane. There are many stationary configurations without cusps and one with two cusps, which are located above and below the equatorial plane.
5. $\lambda_{\text{ms}} < \lambda < \lambda_2$ (Fig. 2, bottom left panel). W has a local minimum located on the equatorial plane at a radius larger than the one of the marginally stable orbit. There are many stationary configurations without cusps and one with two cusps, which are located above and below the equatorial plane.
6. $\lambda = \lambda_2$ (Fig. 2, bottom right panel). The equipotential surface with the two cusps is the one with $W = 0$. Accretion is possible in the limit of a disk of infinite size.
7. $\lambda > \lambda_2$ (Fig. 3). No accretion is possible, as there are no equipotential surfaces $W \leq 0$ with cusps.

Unfortunately, λ_1 and λ_2 are found numerically and, unlike λ_{ms} and λ_{mb} , there is apparently not a simple interpretation of them in term of the λ of a free particle. Let us also note that, as pointed out in Refs. [34–36], the topology of the event horizon of these BHs may be non-trivial. In Fig. 1, the BH horizon has the topology of a torus. In Figs. 2 and 3, it has the topology of two 2-spheres.

3.2 Exotic compact objects without horizon in General Relativity

The Manko-Mielke-Sanabria-Gómez (MMS) metric [44] is an exact solution of the Einstein-Maxwell equations. It can describe the exterior gravitational field around an exotic compact object. The equation of state of ordinary matter cannot explain very compact objects exceeding $3 M_\odot$ and for this reason here we include the word “exotic”. We consider the version with three parameters: the mass M , the specific spin angular momentum $a = J/M$, and the parameter b . In Ref. [44], the metric was written in prolate spheroidal coordinates, which are suitable only for slow-rotating compact objects. It was extended to objects with spin parameter larger than 1 in Ref. [31], by a coordinate transformation to oblate spheroidal coordinates. As in the next section we are interested in fast-rotating objects, here we write the metric in oblate spheroidal coordinates and we refer to the original paper for the slow-rotating case. The line element is

$$ds^2 = -f(dt - \omega d\phi)^2 + \frac{k^2 e^{2\gamma}}{f}(x^2 + y^2) \left(\frac{dx^2}{x^2 + 1} + \frac{dy^2}{1 - y^2} \right) + \frac{k^2}{f}(x^2 + 1)(1 - y^2) d\phi^2, \quad (3.3)$$

where

$$f = \frac{A}{B}, \quad \omega = -(1 - y^2) \frac{C}{A}, \quad e^{2\gamma} = \frac{A}{16k^8(x^2 + y^2)^4}. \quad (3.4)$$

$k = \sqrt{-d - \delta}$ and

$$\delta = -\frac{M^2 b^2}{M^2 - (a - b)^2}, \quad d = \frac{M^2 - (a - b)^2}{4}. \quad (3.5)$$

The functions A , B , and C can be written in the following compact way [44]

$$A = R^2 + \lambda_1 \lambda_2 S^2, \quad B = A + RP + \lambda_2 ST, \quad C = RT - \lambda_1 SP. \quad (3.6)$$

Here $\lambda_1 = k^2(x^2 + 1)$, $\lambda_2 = y^2 - 1$, and

$$\begin{aligned} P &= 2kMx[(2kx + M)^2 - 2y^2(2\delta + ab - b^2) - a^2 + b^2] - 4y^2(4\delta d - M^2 b^2), \\ R &= 4[k^2(x^2 + 1) + \delta(1 - y^2)]^2 + (a - b)[(a - b)(d - \delta) - M^2 b](1 - y^2)^2, \\ S &= -4\{(a - b)[k^2(x^2 + y^2) + 2\delta y^2] + y^2 M^2 b\}, \\ T &= 8Mb(kx + M)[k^2(x^2 + 1) + \delta(1 - y^2)] + \\ &\quad + (1 - y^2)\{(a - b)(M^2 b^2 - 4\delta d) - 2M(2kx + M)[(a - b)(d - \delta) - M^2 b]\}. \end{aligned} \quad (3.7)$$

The Kerr metric is recovered for $b = \sqrt{a^2 - M^2}$, so b is not the usual deformation parameter which measures deviations from the Kerr geometry.

As in the case of the JP space-time, the hydrodynamical structure of thick accretion disks in the MMS background can be immediately obtained by using the corresponding metric coefficient. The qualitative picture is the same we have already discussed in the JP space-time: we have the Kerr-like scenario of Fig. 1 when the ISCO is set by the orbital stability along the radial direction, and the two-cusps scenario of Figs. 2 and 3 when the ISCO is marginally vertically stable. At this point, a quantitative comparison of the two metrics is not possible, as the parameters ϵ_3 and b have not a clear physical meaning. However, as discussed in the next sections, when we consider observable phenomena, the physically relevant properties are quite similar, despite the completely different origin of the two space-times.

4 Evolution of the spin parameter

An accreting compact object changes its mass and spin angular momentum as a consequence of the accretion process. Solid results of the spin evolution would necessarily require realistic non-stationary models of disks accretion and jet emission. That is not possible at present, and therefore we can just estimate the spin evolution with simple (or very simple) accretion models, whose results have to be taken with some caution. The general picture is that the accreting gas falls to the compact object by losing energy and angular momentum. When it reaches the inner edge of the disk, it plunges onto the compact object. If the gas emits no or negligible additional radiation after having plunged, the mass and the spin of the compact object change by $\delta M = -u_t^{\text{in}} \delta m$ and $\delta J = u_\phi^{\text{in}} \delta m$, where $-u_t^{\text{in}}$ and u_ϕ^{in} are, respectively, the specific energy and the specific angular momentum of the gas's particles at the inner edge of the disk, while δm is the gas rest-mass. The evolution of the spin parameter is thus governed by the following equation:

$$\frac{da_*}{d \ln M} = \frac{\lambda_{\text{in}}}{M} - 2a_* . \quad (4.1)$$

In the case of a thin accretion disk in the Kerr background, λ_{in} is supposed to be λ_{ms} (Novikov-Thorne model) and the equilibrium value of the spin parameter is $a_*^{\text{eq}} = 1$ [45]; that is, the object is spun up by the accretion process if $a_* < 1$, and spun down if $a_* > 1$. Including the effect of the radiation emitted by the disk and captured by the BH, one finds the famous Thorne's limit $a_*^{\text{eq}} = 0.9978$ (when the disk's emission is assumed isotropic) [46], as the radiation with angular momentum opposite to the BH spin has larger capture cross-section. The effect of the returning radiation (the radiation emitted by the disk returning to the disk as a consequence of light bending) introduces a smaller correction to the Thorne's limit and the equilibrium spin parameter changes to $a_*^{\text{eq}} = 0.9983$ [47].

In the case of thick disks, one can note that in the Polish doughnut model the inner edge of the disk is inside the marginally stable orbit and it can be arbitrary close to the marginally bound one: here the radiative efficiency $\eta = 1 + u_t^{\text{in}}$ goes to zero and therefore the spin evolution is very weakly affected by the emission of radiation, suggesting that the Thorne's bound can be exceeded [48]. However, a more detailed calculation requires to include the effect of the fluid's viscosity, which was assumed to be completely negligible in [48]. Very recently, in Ref. [49] the authors have studied the spin evolution for high accretion rates in a relativistic, advective, optically thick slim accretion disk model. They find that the BH spin evolution is hardly affected by the emitted radiation at high accretion rate ($\dot{M} \gtrsim 10\dot{M}_{\text{Edd}}$, where \dot{M}_{Edd} is the Eddington mass accretion rate) and that the equilibrium spin value is determined by the flow properties. For $\dot{M} = 10\dot{M}_{\text{Edd}}$ and a viscosity parameter $\alpha = 0.01$, they get $a_*^{\text{eq}} = 0.9994$ [49].

The spin evolution in non-Kerr space-times (non-Kerr BHs and compact objects without an event horizon) have been discussed in [30–33], but only in the case of accretion from thin disk. The key-result of those papers is that the bound $|a_*| \leq 1$ can be violated. With the results of the previous section, we can here consider the case of thick accretion disks. The Polish doughnut model, in which the viscosity parameter α is supposed to be completely negligible, is surely an extremely simplified model. Moreover, we have studied the case of marginally stable disks with $\lambda = \text{const.}$, which is known to be unstable on a dynamical time-scale (a few orbital periods) [50]. Nevertheless, we believe that our simple prescription can provide the correct insight. These accretion disks become stable for very small values of the angular momentum slope [51]. As shown in [48] in the Kerr background, even here the effect

of the emitted radiation should become negligible for super-Eddington rates³. In the end, our goal is to find a conservative upper limit to the maximum value of the spin parameter of these objects and all our approximations can only overestimate a_*^{eq} , so our final result is indeed conservative. The equilibrium values of the spin parameter as a function of the deformation one are reported in Fig. 4, respectively for the JP (left panel) and MMS (right panel) backgrounds.

5 Discussion

As discussed in [32], the value of the spin parameter of a compact object is determined by the competition of three physical processes: the event creating the object, mergers, and gas accretion. In the case of the super-massive BH candidates at the centers of galaxies, the value of the natal spin is completely irrelevant, as the object has increased its mass by several orders of magnitude and the spin has changed accordingly. Minor mergers and short-term accretion events are random events and the net effect is to spin the compact object down. Major mergers can unlikely produce very-fast rotating objects and therefore the maximum value of the today spin parameter of the super-massive BH candidates in galactic nuclei is likely a_*^{eq} , which is reached after long-term accretion from a disk. Let us note that this is true even if the initial spin parameter is higher than a_*^{eq} , as in this case the long-term accretion processes (and, even more efficiently, the other accretion mechanisms) would spin the compact object down to a_*^{eq} . With this observation, we can exclude the region on the right hand side of the curve a_*^{eq} on the plane spin-deformation parameter, see Fig. 4.

The left hand side of the spin-deformation parameter plane can be constrained by current spin measurements, which are usually obtained by assuming the Kerr background. At present, the two most popular and reliable approaches are the continuum-fitting method (see e.g. [40, 52, 53] and references therein) and the analysis of the $K\alpha$ iron line (for a review, see e.g. [54]). The continuum-fitting method infers the spin value by studying the thermal spectrum of a thin accretion disk. As discussed in Refs. [12, 20, 23, 25], actually this technique measures the radiative efficiency of the Novikov-Thorne model, $\eta_{\text{NT}} = 1 + u_t^{\text{ms}}$. It is thus easy to translate a spin measurement under the Kerr assumption into an allowed region on the spin-deformation parameter plane. For instance, the spin of the stellar-mass BH candidate in GRS 1915+105 has been estimated $a_* > 0.98$ in [55]. Such a measurement corresponds to $\eta_{\text{NT}} > 0.234$ in terms of the radiative efficiency of the Novikov-Thorne model. However, the continuum-fitting method can be applied only to stellar-mass BH candidates: the temperature of the disk is proportional to $M^{-1/4}$ and therefore the disk's peak is around 1 keV for an object with $M \sim 10 M_\odot$, but in the UV range for a super-massive BH candidate. In the latter case, dust absorption prevents a spin measurement. On the contrary, our argument is true only for super-massive BH candidates. In the case of stellar-mass objects in X-ray binaries, the spin more likely reflects the value at the time of formation of the BH candidate. The accretion disk originates from the material stripped from the stellar companion. If the latter is massive ($M \gtrsim 10 M_\odot$), its lifetime is too short to alter significantly the mass and the spin of the BH candidate, even assuming an accretion rate at the Eddington limit. If the stellar companion has a mass $M \sim M_\odot$, even after swallowing the whole star the mass and the spin of the BH candidate cannot change significantly.

³Let us note that, even when $\lambda \rightarrow \lambda_2$, the radiative efficiency $\eta = 1 + u_t^{\text{in}} \rightarrow 0$ and therefore the emitted radiation is likely irrelevant.

The study of the shape of the $K\alpha$ iron line can instead probe the space-time geometry of both stellar-mass and super-massive BH candidates. In the case of the super-massive BH candidates, there are at least two objects that seem to rotate quite fast: for both MGC-6-30-15 and 1H 0707-495, the spin has been estimated $a_* > 0.98$, respectively in Ref. [56] and Ref. [57]. The information on the space-time geometry in the $K\alpha$ iron line have been discussed quite in detail in Ref. [28]. Unlike the continuum-fitting method, in this case it seems there is no simple recipe to translate a spin measurement under the Kerr background hypothesis into an allowed region on the spin-deformation parameter plane. Despite that, we can anyway say that the correlation between spin and deformation parameter in the profile of the $K\alpha$ iron line is not too different from the one of the disk’s thermal spectrum. So, the combination of the spin measurements from the continuum-fitting method and the $K\alpha$ iron line of the same object can test the Kerr-nature of a BH candidate only if the two measurements are quite good (for this purpose, the use of the jet power discussed in [23, 25] would be more efficient, but the problem is that the exact mechanism responsible for the production of jets is not yet clear). For instance, in Ref. [58], the authors consider the stellar-mass BH candidate XTE J1550-564. They find $a_* = 0.34$ ($-0.11 < a_* < 0.71$ at 90% C.L.) from the continuum-fitting method, and $a_* = 0.55^{+0.15}_{-0.22}$ from the analysis of the relativistic $K\alpha$ iron line. In Ref. [28], one of us considered as example the $K\alpha$ iron line generated around a JP BH with $a_* = 0.20$ and $\epsilon_3 = 7$, which is a quite deformed object. It turns out that such a JP BH has a thermal spectrum indistinguishable from a Kerr BH with $a_* = 0.68$ and a $K\alpha$ iron line indistinguishable from a Kerr BH with $a_* = 0.47$ (see section IV.B and Fig. 9 of Ref. [28]). Here for “indistinguishable” we do not mean it cannot be distinguished by current X-ray measurements, but that the difference is really negligible and indeed impossible to detect even in the foreseeable future. So, the combination of two different techniques is surely the only way to test the Kerr-nature of BH candidates, and the combination of the continuum-fitting method and of the $K\alpha$ iron line is likely the best option for the near future, but current measurements are not really good enough to put interesting constraints.

A third method potentially capable of providing a mean value of the spin parameter of super-massive BH candidates is based on the Soltan’s argument [59], which relates the mean BH mass density with the mean energy density radiated by super-massive BHs in the current Universe. The argument provides an estimate of the mean radiative efficiency η . However, within a simple disk model which neglects jet emission and other non-thermal phenomena, the maximum radiative efficiency is the one of the Novikov-Thorne model, $\eta_{\text{NT}} = 1 + u_t^{\text{ms}}$. For most objects, this should provide a conservative estimate, as the actual value is likely lower. So, an estimate of η could provide a lower bound for a_* . There are several sources of uncertainty in the final result, but a mean radiative efficiency $\eta > 0.15$ seems to be a conservative lower limit [60]. For instance, the authors of Ref. [61] find a mean radiative efficiency $\eta \approx 0.30 - 0.35$ without some important assumptions necessary in the original version of the Soltans argument.

As here we are interested in a conservative bound on the maximum value of the spin parameter of the super-massive BH candidates, we can adopt the observational constraint $\eta > 0.15$ from the Soltan’s argument. The mean radiative efficiency of AGNs claimed in Ref. [61] or the analyses of the $K\alpha$ iron line of the BH candidates MGC-6-30-15 and 1H 0707-495 would clearly provide a stronger bound in our study. Even if these AGNs are accreting from a thin disk, they may have experienced a period of super-Eddington accretion in the recent past, and the value of their spin parameter may be between the equilibrium value of a

Bound	JP background		MMS background	
	Thin disks	Thick disks	Thin disks	Thick disks
$\eta > 0.15$	$ a_* < 1.196$	$ a_* < 1.292$	$ a_* < 1.179$	$ a_* < 1.312$
$\eta > 0.20$	$ a_* < 1.100$	$ a_* < 1.169$	$ a_* < 1.090$	$ a_* < 1.193$
$\eta > 0.25$	$ a_* < 1.047$	$ a_* < 1.092$	$ a_* < 1.040$	$ a_* < 1.121$

Table 1. Constraints on the spin parameter of the super-massive BH candidates in galactic nuclei from thin and thick accretion disks, for the case of JP and MMS backgrounds.

thin disk and the one of a thick disk. The allowed region on the spin-deformation parameter plane is thus the overlap region determined by the bounds $\eta > 0.15$ and $a_* < a_*^{\text{eq, thick}}$, shown in Fig. 4. The maximum value for the spin is

$$a_*^{\text{max}} \approx 1.3, \quad (5.1)$$

for both JP and MMS space-times. Such a bound is only slightly weaker than $a_*^{\text{max}} \approx 1.2$ found in Ref. [32], whose discussion was limited to thin disks. A more detailed list of the possible bounds on a_* , even assuming more stringent constraints on η , is reported in Tab. 1.

As already mentioned above, our argument cannot be directly applied to stellar-mass BH candidates, as the mass gained from accretion is not relevant for these objects and the value of their spin parameter may still reflect the natal one. However, if we believe that stellar-mass BH candidates have been spun up by the quick accretion of the material around them left by the explosion of the progenitor star, the thick accretion disk model might provide even for these objects an estimate of the maximum spin. As there are objects like GRS 1915+105, whose radiative efficiency has been measured to be $\eta > 0.234$, the constrain on a_*^{max} would be stronger than the one in (5.1), see Tab. 1.

6 Summary and conclusions

A fundamental limit for a BH in 4-dimensional General Relativity is the bound $|a_*| \leq 1$, which is the condition for the existence of the event horizon. However, the process of accretion can spin the object up to a spin value very close to this limit. In the case of a thin accretion disk, the Thorne’s limit is $a_* = 0.9978$ [46]. The accretion process from a thick disk may be more efficient and spins the BH up to a spin value closer to 1. In this work, we have considered the possibility that astrophysical BH candidates are not the BHs predicted by General Relativity, which is not in conflict with current observations, as the nature of these objects has still to be verified. We have studied the accretion process from thick disks in the Polish doughnut framework with constant angular momentum λ . The picture of the accretion process may be qualitatively different from the one in the Kerr background, as the marginally bound orbit may not exist. The disk may have two cusps, one above and one below the equatorial plane, and the gas may plunge onto the compact object from the cusps to the poles of the compact object. We have then estimated the equilibrium value of the spin parameter of these non-Kerr objects as a function of their deformation parameter. Finally, considering that the radiative efficiency of AGNs should be $\eta > 0.15$, we used the argument of Ref. [32] to conclude that the maximum value of the today spin parameter of the super-massive BH candidates at the

centers of galaxies is

$$a_*^{\max} \approx 1.3. \quad (6.1)$$

While we have no rigorous proof of this bound, we think it does not depend very much on the exact background metric: a quite similar constraint was obtained considering two different space-times, suggesting that it may hold regardless of the exact nature of these objects.

Acknowledgments

We thank Shiyi Xiao for useful discussions and suggestions. This work was supported by the Thousand Young Talents Program and Fudan University.

References

- [1] B. Carter, *Phys. Rev. Lett.* **26**, 331 (1971).
- [2] D. C. Robinson, *Phys. Rev. Lett.* **34**, 905 (1975).
- [3] P. T. Chrusciel, J. L. Costa and M. Heusler, *Living Rev. Rel.* **15**, 7 (2012) [arXiv:1205.6112 [gr-qc]].
- [4] R. Penrose, *Riv. Nuovo Cim. Numero Speciale* **1**, 252 (1969) [*Gen. Rel. Grav.* **34**, 1141 (2002)].
- [5] P. S. Joshi and D. Malafarina, *Int. J. Mod. Phys. D* **20**, 2641 (2011) [arXiv:1201.3660 [gr-qc]].
- [6] E. Barausse, V. Cardoso and G. Khanna, *Phys. Rev. Lett.* **105**, 261102 (2010) [arXiv:1008.5159 [gr-qc]].
- [7] E. Barausse, V. Cardoso and G. Khanna, *Phys. Rev. D* **84**, 104006 (2011) [arXiv:1106.1692 [gr-qc]].
- [8] G. Dotti, R. J. Gleiser, I. F. Ranea-Sandoval and H. Vucetich, *Class. Quant. Grav.* **25**, 245012 (2008) [arXiv:0805.4306 [gr-qc]].
- [9] P. Pani, E. Barausse, E. Berti and V. Cardoso, *Phys. Rev. D* **82**, 044009 (2010) [arXiv:1006.1863 [gr-qc]].
- [10] R. Narayan, *New J. Phys.* **7**, 199 (2005) [gr-qc/0506078].
- [11] C. Bambi, *Mod. Phys. Lett. A* **26**, 2453 (2011) [arXiv:1109.4256 [gr-qc]].
- [12] C. Bambi, arXiv:1301.0361 [gr-qc].
- [13] L. Barack and C. Cutler, *Phys. Rev. D* **75**, 042003 (2007) [gr-qc/0612029].
- [14] T. A. Apostolatos, G. Lukes-Gerakopoulos and G. Contopoulos, *Phys. Rev. Lett.* **103**, 111101 (2009) [arXiv:0906.0093 [gr-qc]].
- [15] G. Lukes-Gerakopoulos, T. A. Apostolatos and G. Contopoulos, *Phys. Rev. D* **81**, 124005 (2010) [arXiv:1003.3120 [gr-qc]].
- [16] C. Bambi and K. Freese, *Phys. Rev. D* **79**, 043002 (2009) [arXiv:0812.1328 [astro-ph]].
- [17] T. Johannsen and D. Psaltis, *Astrophys. J.* **716**, 187 (2010) [arXiv:1003.3415 [astro-ph.HE]].
- [18] C. Bambi and N. Yoshida, *Class. Quant. Grav.* **27**, 205006 (2010) [arXiv:1004.3149 [gr-qc]].
- [19] T. Johannsen and D. Psaltis, *Astrophys. J.* **726**, 11 (2011) [arXiv:1010.1000 [astro-ph.HE]].
- [20] C. Bambi and E. Barausse, *Astrophys. J.* **731**, 121 (2011) [arXiv:1012.2007 [gr-qc]].
- [21] C. Bambi, *Phys. Rev. D* **83**, 103003 (2011) [arXiv:1102.0616 [gr-qc]].

- [22] S. Chen and J. Jing, Phys. Lett. B **711**, 81 (2012) [arXiv:1110.3462 [gr-qc]].
- [23] C. Bambi, Phys. Rev. D **85**, 043002 (2012) [arXiv:1201.1638 [gr-qc]].
- [24] S. Chen and J. Jing, Phys. Rev. D **85**, 124029 (2012) [arXiv:1204.2468 [gr-qc]].
- [25] C. Bambi, Phys. Rev. D **86**, 123013 (2012) [arXiv:1204.6395 [gr-qc]].
- [26] H. Krawczynski, Astrophys. J. **754**, 133 (2012) [arXiv:1205.7063 [gr-qc]].
- [27] C. Bambi, Astrophys. J. **761**, 174 (2012) [arXiv:1210.5679 [gr-qc]].
- [28] C. Bambi, Phys. Rev. D **87**, 023007 (2013) [arXiv:1211.2513 [gr-qc]].
- [29] C. Bambi and G. Lukes-Gerakopoulos, arXiv:1302.0565 [gr-qc].
- [30] C. Bambi, Europhys. Lett. **94**, 50002 (2011) [arXiv:1101.1364 [gr-qc]].
- [31] C. Bambi, JCAP **1105**, 009 (2011) [arXiv:1103.5135 [gr-qc]].
- [32] C. Bambi, Phys. Lett. B **705**, 5 (2011) [arXiv:1110.0687 [gr-qc]].
- [33] C. Bambi, Phys. Rev. D **85**, 043001 (2012) [arXiv:1112.4663 [gr-qc]].
- [34] F. Caravelli and L. Modesto, Class. Quant. Grav. **27**, 245022 (2010) [arXiv:1006.0232 [gr-qc]].
- [35] C. Bambi and L. Modesto, Phys. Lett. B **706**, 13 (2011) [arXiv:1107.4337 [gr-qc]].
- [36] C. Bambi, F. Caravelli and L. Modesto, Phys. Lett. B **711**, 10 (2012) [arXiv:1110.2768 [gr-qc]].
- [37] M. Kozłowski, M. Jaroszynski and M. Abramowicz, Astron. Astrophys. **63**, 209 (1978).
- [38] M. Abramowicz, M. Jaroszynski and M. Sikora, Astron. Astrophys. **63**, 221 (1978).
- [39] I. D. Novikov, K. S. Thorne, “Astrophysics of Black Holes” in *Black Holes*, edited by C. De Witt and B. De Witt (Gordon and Breach, New York, New York, 1973), pp. 343-450.
- [40] J. E. McClintock, R. Narayan, S. W. Davis, L. Gou, A. Kulkarni, J. A. Orosz, R. F. Penna and R. A. Remillard *et al.*, Class. Quant. Grav. **28**, 114009 (2011) [arXiv:1101.0811 [astro-ph.HE]].
- [41] T. Johannsen and D. Psaltis, Phys. Rev. D **83**, 124015 (2011) [arXiv:1105.3191 [gr-qc]].
- [42] C. Bambi and E. Barausse, Phys. Rev. D **84**, 084034 (2011) [arXiv:1108.4740 [gr-qc]].
- [43] C. Bambi, JCAP **1209**, 014 (2012) [arXiv:1205.6348 [gr-qc]].
- [44] V. S. Manko, E. W. Mielke and J. D. Sanabria-Gomez, Phys. Rev. D **61**, 081501 (2000) [gr-qc/0001081].
- [45] J. M. Bardeen, Nature **226**, 64 (1970).
- [46] K. S. Thorne, Astrophys. J. **191**, 507 (1974).
- [47] L. -X. Li, E. R. Zimmerman, R. Narayan and J. E. McClintock, Astrophys. J. Suppl. **157**, 335 (2005) [astro-ph/0411583].
- [48] M. A. Abramowicz and J. P. Lasota, Acta Astron. **30**, 35 (1980).
- [49] A. Sadowski, M. Bursa, M. Abramowicz, W. Kluzniak, J. -P. Lasota, R. Moderski and M. Safarzadeh, Astron. Astrophys. **532**, A41 (2011); [arXiv:1102.2456 [astro-ph.HE]].
- [50] J. A. Font and F. Daigne, Mon. Not. Roy. Astron. Soc. **334**, 383 (2002) [astro-ph/0203403].
- [51] F. Daigne and J. A. Font, Mon. Not. Roy. Astron. Soc. **349**, 841 (2004) [astro-ph/0311618].
- [52] L. Gou, J. E. McClintock, M. J. Reid, J. A. Orosz, J. F. Steiner, R. Narayan, J. Xiang and R. A. Remillard *et al.*, Astrophys. J. **742**, 85 (2011) [arXiv:1106.3690 [astro-ph.HE]].
- [53] A. K. Kulkarni, R. F. Penna, R. V. Shcherbakov, J. F. Steiner, R. Narayan, A. Skadowski, Y. Zhu and J. E. McClintock *et al.*, Mon. Not. Roy. Astron. Soc. **414**, 1183 (2011) [arXiv:1102.0010 [astro-ph.HE]].

- [54] J. M. Miller, *Ann. Rev. Astron. Astrophys.* **45**, 441 (2007) [arXiv:0705.0540 [astro-ph]].
- [55] J. E. McClintock, R. Shafee, R. Narayan, R. A. Remillard, S. W. Davis and L. -X. Li, *Astrophys. J.* **652**, 518 (2006) [astro-ph/0606076].
- [56] L. W. Brenneman and C. S. Reynolds, *Astrophys. J.* **652**, 1028 (2006) [astro-ph/0608502].
- [57] A. C. Fabian, A. Zoghbi, R. R. Ross, P. Uttley, L. C. Gallo, W. N. Brandt, A. Blustin and T. Boller *et al.*, *Nature* **459**, 540 (2009).
- [58] J. F. Steiner, R. C. Reis, J. E. McClintock, R. Narayan, R. A. Remillard, J. A. Orosz, L. Gou and A. C. Fabian *et al.*, *Mon. Not. Roy. Astron. Soc.* **416**, 941 (2011) [arXiv:1010.1013 [astro-ph.HE]].
- [59] A. Soltan, *Mon. Not. Roy. Astron. Soc.* **200**, 115 (1982).
- [60] M. Elvis, G. Risaliti and G. Zamorani, *Astrophys. J.* **565**, L75 (2002) [astro-ph/0112413].
- [61] J. -M. Wang, Y. -M. Chen, L. C. Ho and R. J. McLure, *Astrophys. J.* **642**, L111 (2006) [astro-ph/0603813].

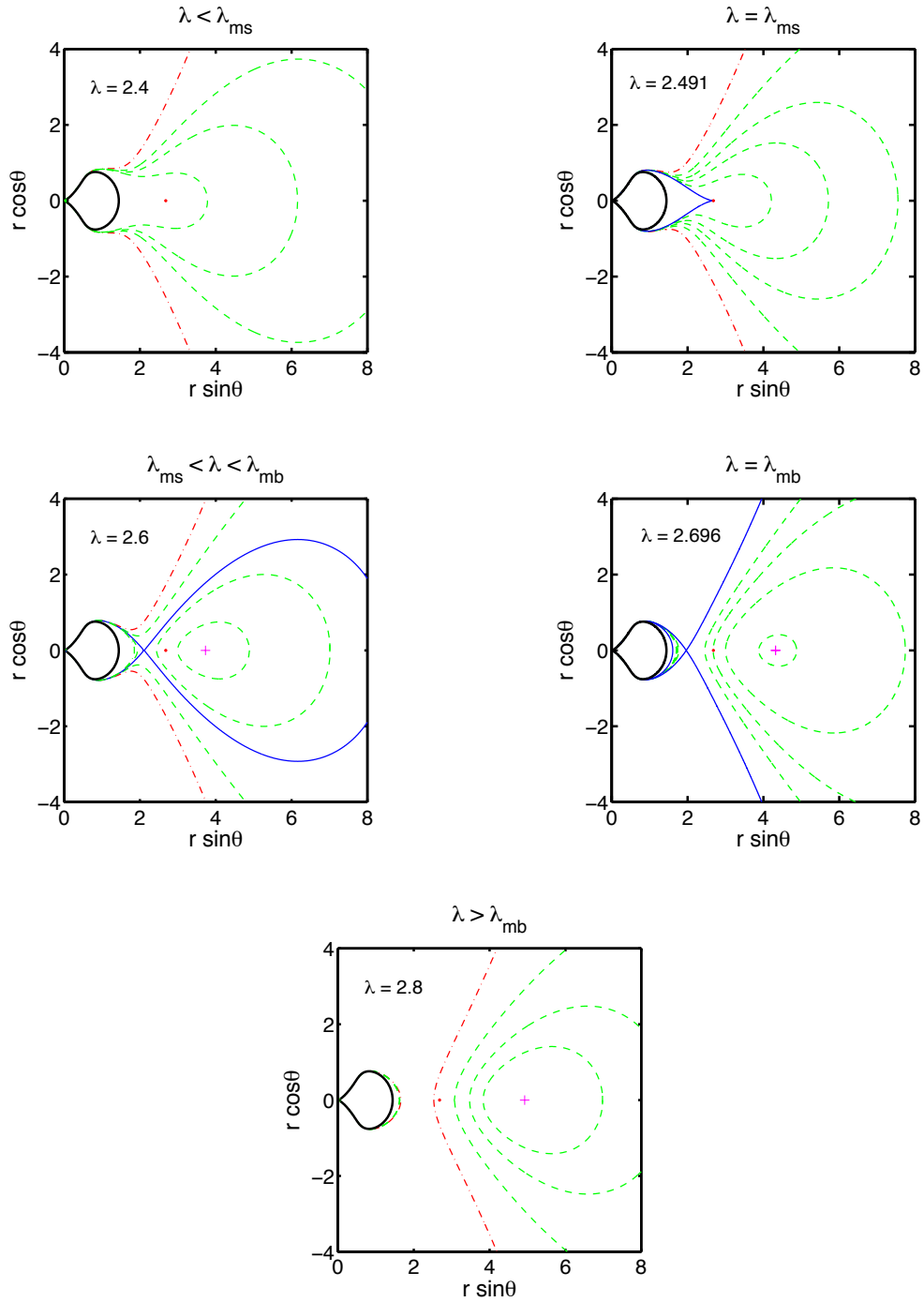


Figure 1. Topology of the equipotential surfaces in the JP background with $a_* = 1.1$ and $\epsilon_3 = -1$. The black solid line is the BH event horizon; the solid blue line is the equipotential surface with the cusp (if any); the dashed green lines are some equipotential surfaces with $W < 0$; the dashed-dotted red line is the equipotential surface $W = 0$; the magenta cross is the local minimum of W (the center of the disk with maximal pressure, if any); the red dot is the location of the marginally stable orbit. Here, $\lambda_{\text{ms}} = 2.491$ and $\lambda_{\text{mb}} = 2.696$. The picture of the accretion process is *qualitatively similar* to the Kerr case.

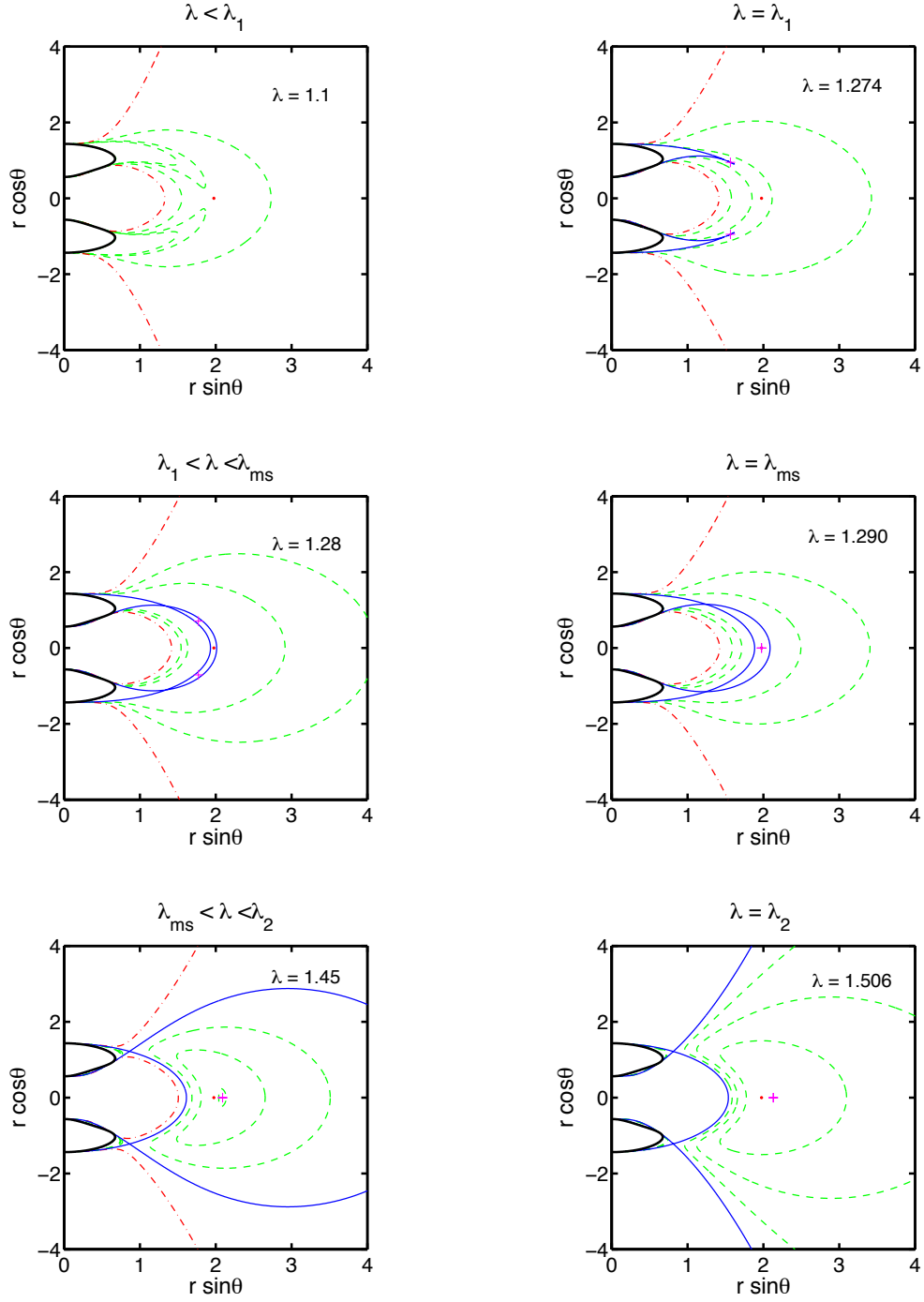


Figure 2. Topology of the equipotential surfaces in the JP background with $a_* = 0.9$ and $\epsilon_3 = 2$. The black solid line is the BH event horizon; the solid blue line is the equipotential surface with the cusps (if any); the dashed green lines are some equipotential surfaces with $W < 0$; the dashed-dotted red line is the equipotential surface $W = 0$; the magenta crosses are the local minima of W (the centers of the disk with maximal pressure, if any); the red dot is the location of the marginally stable orbit. Here, $\lambda_1 = 1.274$, $\lambda_{\text{ms}} = 1.290$, and $\lambda_2 = 1.506$. The picture of the accretion process is *qualitatively different* from the Kerr case.

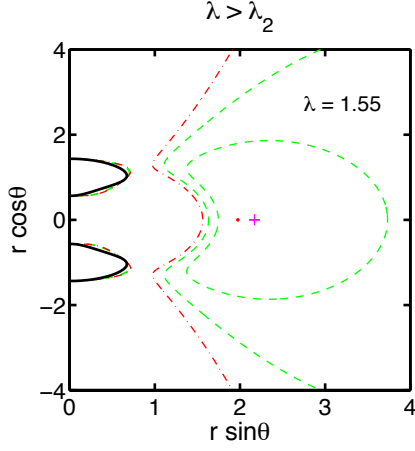


Figure 3. As in Fig. 2 for $\lambda > \lambda_2$.

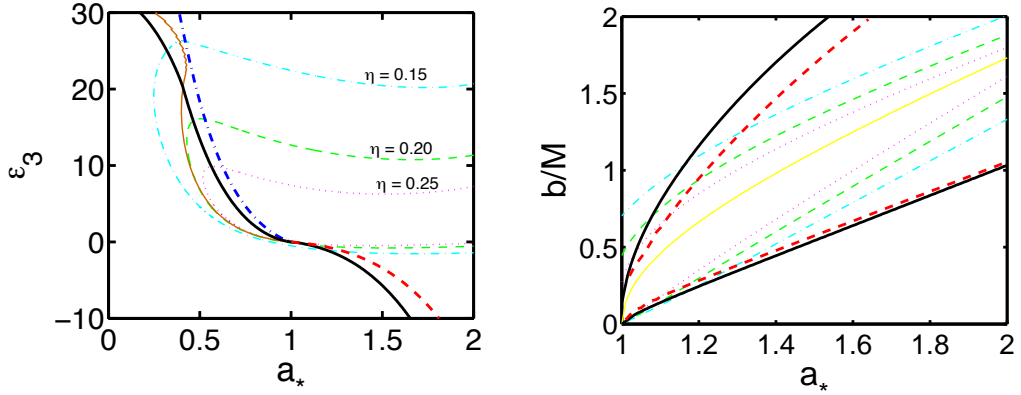


Figure 4. Spin parameter-deformation parameter plane. Curve of a_*^{eq} from accretion from a thick disk (thick dashed red curve for $\lambda = \lambda_{\text{mb}}$ and thick dashed-dotted blue curve for $\lambda = \lambda_2$), curve of a_*^{eq} from accretion from a thin disk (thick solid black curve), Novikov-Thorne radiative efficiency $\eta_{\text{NT}} = 0.15$ (thin dashed-dotted light blue curve), 0.20 (thin dashed green curve), and 0.25 (thin dotted magenta curve). The thin solid brown curve (left panel) for $\epsilon_3 > 0$ separates the regions of the plane in which the ISCO is marginally vertically (right side) and marginally radially (left side) stable. For $b = M\sqrt{a_*^2 - 1}$ (thin solid yellow curve in the right panel), we recover the Kerr solution. Left panel: JP background. Right panel: MMS background.